Supporting information

Design of Specific Inhibitors of Quinolinate Synthase based on [4Fe-4S] Cluster Coordination

Jaione Saez Cabodevilla[a,b], Anne Volbeda[c], Olivier Hamelin[a], Jean-Marc Latour[a], Océane Gigarel[c], Martin Clémancey[a], Claudine Darnault[c], Debora Reichmann[a#], Patricia Amara[c], Juan C. Fontecilla-Camps[c] and Sandrine Ollagnier de Choudens[a*]

[a] Univ. Grenoble Alpes, CEA, CNRS, BIG-LCBM, UMR5249, 38000, Grenoble, France
[b] Univ. Grenoble Alpes, CNRS, ICMG FR 2607, Département de Pharmacochimie Moléculaire, F-38041, Grenoble, France
[c] Univ. Grenoble Alpes, CEA, CNRS, IBS, Metalloproteins, F-38000 Grenoble, France
[#] Wachholtzstr. 2, 38106 Braunschweig, Germany

Corresponding author

Sandrine Ollagnier, Email: sollagnier@cea.fr

Table of contents

1-Materials and Methods

1.1 Chemicals. All the materials necessary for the experiments, namely, dimercaptobenzene (DMB), mercaptobenzene (MB), 4-hydroxyphthalic acid (4HP), 4-aminophthalic acid (4AP), 3-hydroxyphthalic acid (3HP), phthalic acid (PA), quinolinic acid (QA), $MnCl_2$, Citrate, $NADP^+$, isocitrate dehydrogenase, fumarate, L-aspartate and DHAP were purchased from Sigma-Aldrich. 4-mercaptophthalic acid (4MP) was purchased from ChemSpace society (Latvia) and 4,5 dithiohydroxyphthalic acid was purchased from OriBasePharma (Montpellier, France) company as mentioned in reference 1.[1, 2] 5-mercaptopyridine- 2, 3-dicarboxylic acid (5MPDC) was synthetized in our laboratory as already described.[3] 6-chloropyridine-2,3-dicarboxylic acid dimethyl ester was obtained using reported procedures.[4-6]

1.2 Synthesis of 6MPDC and 5MPzDC

1.2. a) 6-mercaptopyridine- 2, 3-dicarboxylic acid (6MPDC)

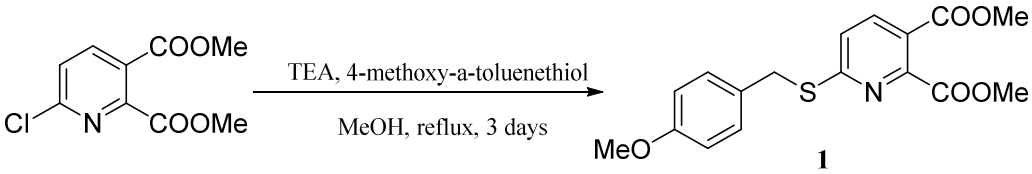

6- ((4- methoxybenzyl)thio) pyridine- 2, 3- dicarboxylic acid dimethyl ester (1). To a solution of triethylamine (4.12 mL, 29.6 mmol) in methanol (90 mL) previously deoxygenated by argon bubbling for 10 min, α-methoxytoluenethiol (4.12 mL, 29.6 mmol) and 6- chloropyridine- 2, 3- dicarboxylic acid dimethyl ester (3.40 g, 14.8 mmol) were added. The resulting mixture was refluxed for three days, diluted with water and extracted with EtOAc (x3). The organic layers were combined, washed with brine, dried over $MgSO_4$ and concentrated *in vacuo*. Purification of the residue by column chromatography (2 % $MeOH/CH_2Cl_2$) gave the tittle compound as a white-yellow powder in 53% yield (7.78 g).
RMN ^1H (300 MHz, $CDCl_3$): δ 8.00 (d, *J* = 8.4 Hz, 1H), 7.34 (d, *J* = 8.7 Hz, 2H), 7.25 (d, *J* = 8.4 Hz, 1H), 6.84 (d, *J* = 8.7 Hz, 2H), 4.44 (s, 2H), 4.03 (s, 3H), 3.91 (s, 3H), 3.80 (s, 3H). RMN ^{13}C (75 MHz, $CDCl_3$): δ 167.1 (C), 165.1 (C), 164.2 (C), 158.9 (C), 152.0 (C), 137.0 (CH), 130.3 (2 CH), 129.0 (C), 122.3 (CH), 119.8 (C), 114.0 (2 CH), 55.3 (CH_3), 52.9 (CH_3), 52.6 (CH_3), 34.1 (CH_2). MS (m/z, ESI)**:** Calcd. for $[C_{17}H_{17}NO_5S+H^+]^+$: 348.1; Found: 348.0.

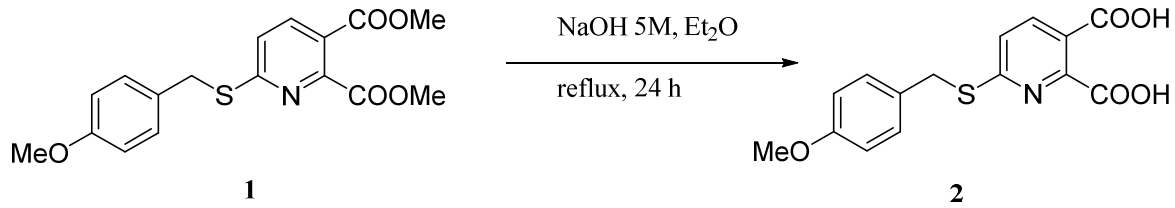

6- ((4- methoxybenzyl)thio) pyridine- 2,3 -dicarboxylic acid (2). To a solution of **1** (2.56 g, 7.37 mmol) in Et_2O (14 mL), an aqueous solution of 5 M NaOH (14 mL) was added. The mixture was refluxed for 24 h then cooled to room temperature. After acidification of the solution to pH 2.0 by dropwise addition of concentrated HCl, the product was extracted with EtOAc (x3). The combined organic layers were dried over Na_2SO_4 and concentrated *in vacuo*. The resulting residue was washed several times with acetone to afford the tittle compound as a white solid in 94 % yield (2.21 g).
RMN ^1H (300MHz, acetone-d6): δ 8.12 (d, *J* = 8.5 Hz, 1H), 7.46 (d, *J* = 8.5 Hz, 1H), 7.41 (d, *J* = 8.5 Hz, 2H), 6.86 (d, *J* = 8.5 Hz, 2H), 4.47 (s, 2H), 3.77 (s, 3H). RMN ^{13}C (75 MHz, acetone-d6): δ 166.7 (C), 165.2 (C), 163.2 (C), 159.1 (C), 152.6 (C), 137.8 (CH), 130.3 (2 CH), 129.3 (C), 122.1 (CH), 120.5 (C), 113.8 (2 CH), 54.6 (OCH_3),

33.3 (CH_2). MS (m/z), ESI): Calcd. for $[C_{15}H_{13}NO_5S\text{-}H^+]^-$: 318.0; Found: 317.9, Calcd. for $[C_{15}H_{13}NO_5S\text{-}H^+\text{-}CO_2]^-$: 274.1; Found: 273.9, Calcd. for $[C_{15}H_{13}NO_5S\text{-}H^+\text{-}2CO_2]^-$: 230.1; Found: 229.9.

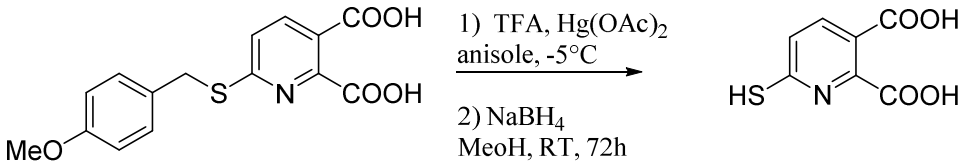

2 **6MPDC**

6-mercaptopyridine- 2, 3-dicarboxylic acid[7] **(6MPDC).** A mixture of **2** (2.00 g, 6.33 mmol) and anisole (40 mL) was cooled to -5°C in a water-ice-NaCl bath. Trifluoroacetic acid (200 mL) and mercury (II) acetate (2.07 g, 6.52 mmol) were added. The reaction mixture was stirred for 1 h at -5 °C and then concentrated under reduced pressure to afford an orange oil. The product was precipitated as a white solid by addition of a 1:1 water-Et_2O mixture to the residue. After filtration and drying under vacuum, the resulting solid was allowed to react with sodium borohydride (0.48 g, 12.66 mmol) in MeOH (150 mL) for 72 h. Next, the resulting mixture was cooled to 0°C and cautiously quenched by slow addition of concentrated HCl to pH= 2-3. After dilution with water, the product was extracted with EtOAc (x3). The organics were combined, dried over Na_2SO_4, and concentrated to the fifth. The title compound 6MPDC was obtained by precipitation in a large volume of hexane in 20% yield (250 mg, 1.27 mmol).
RMN ^1H (300MHz, acetone-d6): δ 7.89 (dd, *J* = 8.5, 4.5 Hz, 1H), 7.41 (dd, *J* = 8.5, 4.5 Hz, 1H); RMN ^{13}C (75 MHz, acetone-d6): δ 170.9 (C), 165.2 (C), 165.1 (C), 149.5 (C), 138.1 (CH), 126.5 (CH), 119.5 (C). MS (m/z, ESI): Calcd. for $[C_7H_5NO_4S\text{-}H^+]^-$: 198.0; Found: 197.9. HRMS (m/z, ESI): Calcd. for $[C_7H_5NO_4S\text{-}H^+]^-$: 197.98665; Found: 197.98689

1.2.b) Synthesis of 5-mercaptopyrazine 2,3-dicarboxylic acid (5MPzDC)

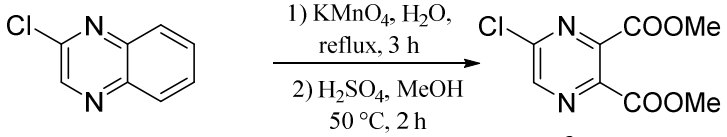

3

5-chloropyrazine- 2, 3- dicarboxylic acid dimethyl ester (3). 5-chloropyrazine -2, 3- dicarboxylic acid was obtained from 2-chloroquinoxaline using reported procedure in similar yield.[8] A solution of $KMnO_4$ (24.00 g, 151.9 mmol) in H_2O (250 mL) was added dropwise within 2 h to a refluxing solution of 2-chloroquinoxaline (5.00 g, 30.4 mmol) in H_2O (250 mL). Next, the mixture was refluxed for an additional hour and cooled to 60 °C to filtrate off the MnO_2 over Celite, which was rinsed with hot water (2 x 80 mL). The filtrate was concentrated to about 80 mL and acidified with concentrated HCl to pH 0, and the solvent was then evaporated. The crude 5-chloropyrazine -2, 3- dicarboxylic acid was engaged in the next step without further purification.[8] Concentrated H_2SO_4 (1.00 mL, 18.7 mmol) was added dropwise within 5 minutes to a solution of the residue in MeOH (13 mL) cooled to 0 °C. The resulting mixture was heated at 50 °C for 2 h and stirred at room temperature for additional 3 h. After concentration under reduced pressure, the resulting residue was basified with saturated aqueous $NaHCO_3$ solution to pH ≈ 8 and extracted with EtOAc (x3). The combined organic fractions were dried over anhydrous Na_2SO_4, concentrated *in vacuo* and the residue purified by silica gel column chromatography (2% MeOH/CH_2Cl_2) affording the desired compound as a brown solid in 35% yield over two steps (2.44g).
RMN ^1H (300 MHz, $CDCl_3$): δ 8.77 (1H), 4.05 (s, 6H).RMN ^{13}C (75MHz, $CDCl_3$): δ 163.8 (C), 163.6 (C), 150.5 (C), 145.6 (CH), 145.0 (C), 141.9 (C), 53.7 (CH_3), 53.6 (CH_3). MS (m/z, ESI): Calcd. for $[C_7H_4ClN_2O_3\text{+}H^+]^+$: 200.0; Found: 198.9; Calcd. for $[C_8H_7ClN_2O_4\text{+}H^+]^+$: 231.0 ; Found: 230.9

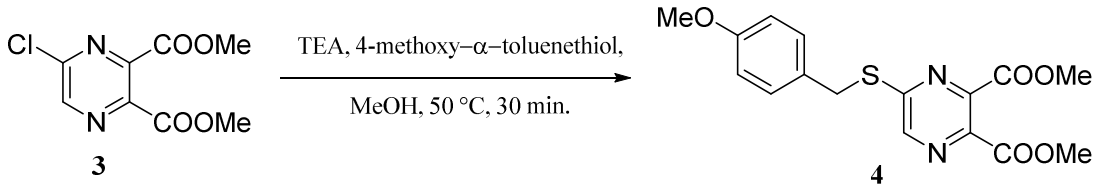

3 4

5-((4-methoxybenzyl)thio)pyrazine-2,3-dicarboxylic acid dimethyl ester (4). A solution of **3** (2.28 g, 9.92 mmol) in MeOH (70 mL) was deoxygenated by argon bubbling for 10 min. Next, triethylamine (1.38 mL, 9.92 mmol) and 4-methoxy-α-toluenethiol (1.38 mL, 9.92 mmol) were added and the resulting solution was heated at 50 °C for 30 min under inert atmosphere. After dilution with water, the product was extracted with EtOAc (x3). The organics were combined, dried over anhydrous Na_2SO_4 and the solvent was evaporated under reduced pressure. The obtained residue was purified by silica gel column chromatography (5 % MeOH/CH_2Cl_2) to afford the tittle compound as a yellow oil in 97 % yield (3.35 g).
RMN ^{1}H (300 MHz, $CDCl_3$): δ 8.49 (s, 1H), 7.32 (d, *J* = 8.0 Hz, 2H), 6.83 (d, *J* = 8.0 Hz, 2H), 4.04 (s, 3H), 3.98 (s, 3H), 3.78 (s, 3H). RMN ^{13}C (75 MHz, $CDCl_3$): δ 165.5 (C), 164.4 (C), 160.5 (C), 159.2 (C), 146.5 (C), 143.4 (CH), 136.4 (C), 130.4 (2 CH), 127.9 (C), 114.1 (2 CH), 55.2 (CH_3), 53.2 (CH_3), 53.2 (CH_3), 33.9 (CH_2). MS (m/z, ESI): Calcd. for $[C_{16}H_{16}N_2O_5S+H^+]^+$: 349.1; Found: 348.9

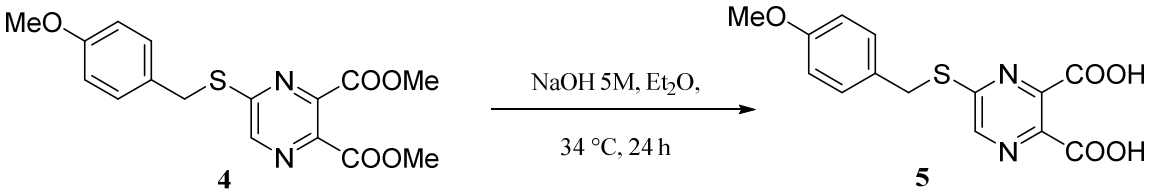

4 5

5-((4 methoxybenzyl)thio)pyrazine-2,3-dicarboxylic acid (5). A 5 M aqueous solution of NaOH (3.15 mL) was added to a solution of **4** (0.575 g, 1.65 mmol) in Et_2O (3 mL). The mixture was refluxed for 24 h then acidified to pH 2 by dropwise addition of concentrated HCl. Next, the solution was extracted with EtOAc (x3) and the combined organic layers were dried over anhydrous Na_2SO_4 and concentrated *in vacuo*. From the residue, the product was extracted with acetone and the resulting solution dried over anhydrous Na_2SO_4, then concentrated under vacuum to give the tittle compound as a dark orange oil in 85 % yield (0.448 g).
RMN ^{1}H (300 MHz, acetone-d6): δ 8.68 (s, 1H), 7.46 (d, *J* = 7.2 Hz, 2H), 6.89 (d, *J* = 7.2 Hz, 2H), 4.54 (s, 2H), 3.79 (s, 3H). RMN ^{13}C (75 MHz, acetone-d6): δ 165.1 (C), 164.5 (C), 159.6 (C), 159.3 (C), 145.8 (C), 143.2 (CH), 137.8 (C), 130.5 (2 CH), 128.6 (C), 113.9 (2 CH), 54.6 (CH_3), 33.1 (CH_2). MS (m/z, ESI)**:** Calcd. for $[C_{14}H_{12}N_2O_5S-H^+]^-$: 319.0; found: 318.9 .

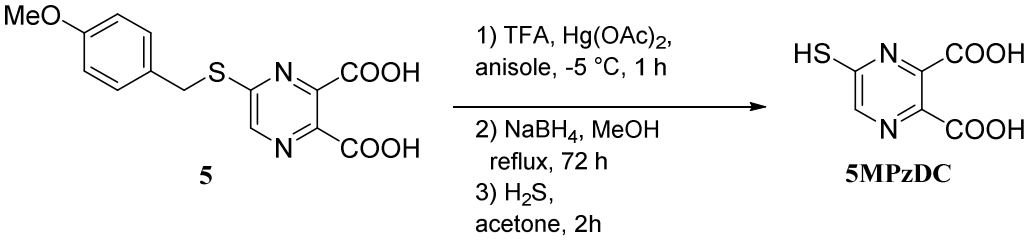

5 **5MPzDC**

5- mercaptopyrazine-2,3-dicarboxylic acid[7] (5MPzDC). Trifluoroacetic acid (90 mL) and mercury (II) acetate (0.535 g, 1.68 mmol) were added to a mixture of **5** (0.448 g, 1.4 mmol) and anisole (9 mL) cooled to -5º C. The reaction mixture was stirred for 1 h at -5 °C. The mixture was concentrated under vacuum to afford an orange oil. Addition of a 1:1 mixture of water-ether (150 mL) resulted in the precipitation of a fraction of the product. The precipitated solid and the water phase were combined and the resulting suspension was concentrated in vacuo. The recovered solid was allowed to react with $NaBH_4$ (0.106 g, 2.8 mmol) in refluxing MeOH (80 mL) for 72 h. After cooling to 0 °C, the resulting mixture was hydrolyzed by slow addition of concentrated HCl to pH≈ 2-3 then concentrated *in vacuo*. The resulting residue was taken up in water and the product extracted with EtOAc (x4). The combined organics layers were concentrated to the fifth and the desired product was precipitated by addition

of the concentrated solution into a large volume of hexane. The resulting residue was solubilized in acetone and H_2S was bubbled at room temperature for 2 hours. After filtration through Celite, the filtrate was concentrated under vacuum to give the desired compound in 55 % yield (0.155 g). Due to a slow degradation of the product, it has to be stored at -80 °C.
RMN ^{1}H (300 MHz, acetone-d6: δ 8.74 (s, 1H) RMN ^{13}C (75 MHz, acetone-d6), δ (ppm): 176.4 (2C), 164.2 (C), 161.5 (C), 157.3 (CH), 136.7 (C). HRMS (m/z, ESI): Calcd. for $[C_6H_4N_2O_4S\text{-}H^+]^-$: 198.98190, Found: 198.98218

1.3 Preparation of *Escherichia coli* [4Fe-4S] NadA. The *Escherichia coli* [4Fe-4S] NadA ([4Fe-4S]-*Ec*NadA) protein was expressed and purified on Ni-NTA affinity column as already described.[9] ^{57}Fe-labelled [4Fe-4S]-*Ec*NadA was prepared as previously reported.[10] Protein concentration was determined by the method of Bradford using bovine serum albumin as standard. It is known that in the case of wild-type *Ec*NadA this method overestimates protein concentration (as determined by the quantitative amino-acid analysis of purified enzyme), therefore a corrective factor of 2.45 was applied. Protein-bound iron concentration was determined under reducing conditions with bathophenanthroline disulfonate after acid denaturation of the protein[11] and the concentration of labile sulfide was measured by the method of Beinert.[12]

1.4 Preparation of *Thermotoga maritima* [4Fe-4S] NadA*Y21F. We call *Tm*NadA* the *Tm*NadA variant that carries the K219R mutation.[3] This mutation allows crystallization of the protein without affecting its biochemical and spectroscopic properties or its *in vivo* and *in vitro* activity.[13] The Y21F variant was generated using *Tm*NadA* as template.[13] Expression and purification of the *Tm*NadA*Y21F variant, as well as introduction of the [4Fe-4S] cluster, were performed as already described.[13] Briefly, purified *Tm*NadA*Y21F (150 µM) was incubated anaerobically with 5 mM DTT for 15 min. Next, 6 molar equivalents of L-cysteine along with catalytic amount of IscS cysteine desulfurase (1.5 µM) and 6 molar equivalents of ferrous iron ($(NH_4)_2Fe(SO_4)_2$) were added. After a 5 h incubation the enzyme was heated for 30 min. at 65°C in the presence of 50 mM DTT. Monomeric [4Fe-4S]-*Tm*NadA was obtained after chromatography through a Superdex-75 column and concentrated to 65 mg/ml for crystallization trials. After reconstitution, a ratio of 3.02 iron and 2.8 sulfur atoms per *Tm*NadA*Y21F monomer was measured.

1.5 Preparation of *Escherichia coli* [4Fe-4S] Aconitase B. The plasmid pG5783 encoding aconitase B (AcnB) was a gift from J.R. Guest (Norwich, UK) and AcnB purification was performed as previously described.[14] After purification *Ec*AcnB contains 0.1-0.2 iron and sulfide per monomer. Its apo-form was obtained by treating the protein with 10 mM EDTA and 10 mM DTT at 4°C overnight and desalting using a Desalting column (Pharmacia). [4Fe-4S]-*Ec*AcnB was obtained by incubating the protein for 3h anaerobically with a 5 molar excess of ferrous iron and sodium sulfide in the presence of 5 mM DTT. After desalting, [4Fe-4S]-*Ec*AcnB containing 3.2-3.5 iron and sulfide per monomer was concentrated and stored at -80°C before use.

1.6 Mossbauer spectroscopy of ^{57}Fe-labeled [4Fe-4S]-*Ec*NadA with inhibitors (6MPDC, 5MPzDC, 5MPDC and 4MP). ^{57}Fe-labeled [4Fe-4S]-*Ec*NadA (175 µM; 3-3.7 iron/protein) was incubated 15 min. in the glove box with 5-5.7 equiv. of 6MPDC, 5MPzDC, 5MPDC and 4MP, transferred to a Mossbauer sample holder, frozen in cooled 2-methyl-butane inside the glove box and kept in liquid nitrogen until the measurement. A control experiment was performed without inhibitor. Mossbauer spectra were recorded at 4.2 K, either on a low-field Mossbauer spectrometer equipped with a Janis SVT-400 cryostat, or on a strong-field Mossbauer spectrometer equipped with an Oxford Instruments Spectromag 4000 cryostat containing an 8T split-pair superconducting magnet. Both spectrometers were operated in a constant acceleration mode in transmission geometry. The isomer shifts are referenced against that of a metallic iron foil at room-temperature. The spectra were analyzed with the program WMOSS (WEB Research, Edina, MN, U.S.A.).
Owing to the similarity of the spectra of [4Fe-4S]-*Ec*NadA alone and in presence of inhibitors developing their reliable simulation was not straightforward. Indeed a balance had to be found between freeing all parameters with the likely risk of overparametrization and using the fewer possible number of parameters with the risk of hiding differences between the Fe sites. Therefore, we increased gradually the number of parameters free to vary and the four iron cluster was successively considered as: (i) the sum of two dimers (delocalized pairs) with different values of IS and QS parameters, (ii) the sum of a group of three identical Fe (with values of the IS and QS parameters fixed at the values obtained by simulation of [4Fe-4S]-*Ec*NadA) and an independent Fe site with singular values of IS and QS parameters (Figure S6 and Table S2), (iii) the sum of a dimer (delocalized pair, with values of the IS and QS parameters fixed at the values obtained by simulation of [4Fe-4S]-*Ec*NadA) and two distinct monomer sites with distinct values of IS and QS parameters (Figure S7 and Table S3), (iv) the sum of a dimer (delocalized pair, with values of the IS and QS parameters allowed to vary) and two distinct monomer sites with distinct values of the IS and QS parameters. The significance of the values of IS and QS parameters was assessed through the change in the least-squares residual χ^2 by varying the parameter around its "best-fit value" over ranges of 0.2 mm

s^{-1} for IS and 0.4 mm s^{-1} for QS. An analysis based on a ca 10 % allowed variation of χ^2 indicated that IS values are estimated with a precision of ± 0.04 mm s^{-1} and QS values with a precision of ± 0.07 mm s^{-1} (Figure S8). Simulation (i) with too few variable parameters failed to reveal any difference between the samples. Simulation (iv) with too many variable parameters led to questionable assignments of the various lines to Fe sites. Simulations (ii) and (iii) proved very consistent with each other leading to congruent conclusions. We prefer simulation (iii) because it appears to us physically more meaningful.

1.7 UV-visible absorption spectroscopy of [4Fe-4S]-*Ec*NadA with inhibitors (6MPDC and 4MP). [4Fe-4S]-*Ec*NadA containing ^{56}Fe (11-21 µM or 300 µM; 2.9-3.2 iron/protein) was used for UV-visible analyses. [4Fe-4S]-*Ec*NadA was incubated inside the glove box with 5 equiv. or 10 equiv. of 6MPDC and 4MP and the reaction monitored after 15 min. incubation using a Uvikon XL (Bio-Tek Instrument) spectrophotometer operating in a dual beam mode. To analyze the interaction of [4Fe-4S]-*Ec*NadA with 4MP and 6MPDC, the data were treated as absorbance vs energy and the absorption maxima were simulated with a Gaussian function to obtain a precise estimation of the absorption maximum.
In order to analyze the interaction of [4Fe-4S]-*Ec*NadA with 4MP, the data were treated as absorbance vs energy and the absorption maxima were simulated with a Gaussian function to obtain a precise estimation of the absorption maximum. The values of the maxima are gathered in Table S4. A similar treatment was applied with 6MPDC but failed to evidence significant differences.

1.8 *In vitro* Aconitase activity. *Ec*AcnB activity was assayed anaerobically according to the procedure described by Gardner and Fridovitch.[15] Briefly, [4Fe-4S]-*Ec*AcnB (0.2 nmol) was incubated anaerobically for 5 min, in a total volume of 100 µl of 50 mM Tris-HCl pH 7.5 buffer, with increasing equivalents of 4-MPA, 6-MPDC, 5-MPZDC and 5-MPDC followed by addition of 25 mM citrate, 0.3 mM $MnCl_2$, 0.5 mM $NADP^+$ and 2.8 µM isocitrate dehydrogenase. The *Ec*AcnB activity was assayed by monitoring the formation of NADPH at 340 nm, which is directly proportional to the formation of isocitrate. A positive control, without inhibitory molecules was also performed and corresponds to the maximal activity of *Ec*AcnB (100%).

1.9 *In vitro* Quinolinate synthase activity. [4Fe-4S]-*Ec*NadA enzymatic activity was assayed under anaerobic conditions as already described with minor changes.[9] Briefly, *Ec*NadA activity inside a glove box at 37°C, was followed by the time-dependent formation of quinolinic acid (QA) measured directly by HPLC. The assay mixture in 100 µl of 50 mM Na-HEPES, 100 mM KCl, pH 7.5 buffer contained 2 mM DHAP, 33 mM L-aspartate, 25 mM fumarate, 10 µM of *Ec*NadB and 10 µM of [4Fe-4S]-*Ec*NadA. In the case of inhibition assays, different concentrations of inhibitory molecules were pre-incubated with the holo-enzyme for 5 min. followed by addition of DHAP, L-aspartate and fumarate. After a further 5 min. preincubation of this assay mixture at 37°C, the reaction was initiated by the addition of 10 µM FAD-containing *Ec*NadB. The reaction was quenched after 20 min by addition of 5 µl 2N H_2SO_4. Precipitated proteins were removed by centrifugation at 15,000 rpm for 15 min. Fifty microliters of the supernatant were injected onto a Tosoh TSK Gel ODS-120T (4.6 mm x 15 cm) column connected to a HP-1100 HPLC system. The QA was eluted with 0.03% TFA, pH 2.4 buffer at a flow rate of 0.5 ml/min. QA was detected by its absorbance at 260 nm and was eluted with a retention time of 9.1 min. After 20 min elution the column was regenerated by applying a linear gradient from 0% to 100% of acetonitrile in 0.03% TFA at 0.5 ml/min for 10 min and re-equilibrated before injection of the next sample. QA was quantified using a standard curve of authentic quinolinic acid (0 to 40 nmol). 100% activity = 0.06 µmol/min/mg.

1.10 Crystallization. All experiments were performed under anaerobic conditions with the *Tm*NadA*Y21F variant, starting from a stock solution with a protein concentration of 65 mg/mL in 50 mM KCl and 100 mM Tris HCl buffer at pH 8.0. The three ligand complexes were prepared as follows.
4MP (4-mercaptopyridine-2,3-dicarboxylic acid) complex. The protein stock solution was diluted inside a glove box to 20 mg/mL in 50 mM KCl and 125 mM Tris HCl at pH 7.2. A volume of 50 µL of this solution was incubated overnight at 20°C with 0.8 µL of 75 mM 4MP in 25 mM Tris HCl at pH 8.0, affording a 1:2 protein-to-ligand ratio. Hanging drops were prepared by mixing one µL of the complex solution with the same volume of a reservoir solution consisting of 26% PEG3350, 100 mM NaCl, 200 mM Na_2HPO_4 and 100 mM MES at pH 6.7 and equilibrated against 1 mL of the latter by vapor diffusion. A plate-shaped brown crystal grew after three weeks in one of these drops. This crystal was transferred to a cryo-protectant solution prepared with 40% PEG3350, 100 mM HEPES pH 7.0, 200 mM Na_2HPO_4 and 100 mM NaCl, flash-cooled anaerobically using liquid propane and immediately stored in liquid nitrogen, as previously described.[16]
6MPDC (6-mercaptopyridine-2,3-dicarboxylic acid) complex. The protein stock solution was diluted inside a glove box to 20 mg/mL by Microcon-10 kDa dialysis in 10 mM Tris HCl pH 8.0. Next, 45 µL of this solution was

incubated overnight at 20°C with 1.3 µL of 50 mM 6MPDC in 10 mM KCl and 50 mM HEPES pH 7.1, giving a 1: 2.6 protein-to-ligand ratio. One µL of the complex solution was mixed with 1 µL of a solution of 26% PEG3350, 1% dioxane, 200 mM Na_2HPO_4 and 100 mM HEPES at pH 7.3 and the resulting hanging drop was equilibrated with 1 mL of the latter reservoir solution. Brown plate-shaped crystals obtained after 2 days were transferred to a cryo-protectant solution of 34% PEG3350, 1% dioxane, 200 mM Na_2HPO_4 and 100 mM HEPES at pH 7.5, flash-cooled and stored as described above for the 4MP complex.

5MPDC (5-mercaptopyridine-2,3-dicarboxylic acid) complex. The protein solution was first diluted inside a glove box to 32.5 mg/mL by Microcon-10 kDa dialysis in 10 mM Tris HCl pH 8.0. 50 µL of this solution was incubated overnight at 20°C with 22 µL of 7.5 mM 5MPDC in 25 mM Tris HCl pH 8.0 and 9.5 µL of 50 mM KCl and 10 mM Tris HCl pH 8.0, to give a 1:3.5 protein-to-ligand ration. One µL of the complex solution was next mixed with 1 µL of a reservoir solution of 24% PEG3350, 2% dioxane, 200 mM Na_2HPO_4 and 100 mM MES pH 6.7. The resulting hanging drop was equilibrated in the vapor phase with 1 mL of the reservoir solution and crystalline brown plates were obtained after 5 days. These were transferred to a cryo-protectant solution of 33% PEG3350, 2% dioxane, 200 mM Na_2HPO_4 and 100 mM HEPES at pH 6.7 and flash-cooled and stored as described above for the *Tm*NadA complexes with 4MP and 6MPDC.

1.11 X-Ray Structure Determination. X-ray diffraction data were collected under cryogenic (≈100 K) conditions at beam lines ID29 and ID30B of the European Synchrotron Radiation Facility in Grenoble, France (Table S1), using the program *MXCuBe*.[17] After indexation, integration and initial scaling with the *XDS* package[18], the data were submitted to a final scaling and merging step with *AIMLESS*[19] of the *CCP4* package.[20] Structures were solved by molecular replacement with *PHASER*[21] using the *Tm*NadA*Y21F-XY complex[3] (pdb code 6F48) as starting model. Manual model corrections were performed with COOT.[22] *REFMAC5*[23] was used to refine individual atomic positions and isotropic temperature factors along with TLS parameters of the three NadA domains and its cluster binding region for the 6MPDC and 5MPDC complexes, whereas the same program was used to refine atomic positions and anisotropic temperature factors for the 4MP complex. Dictionary files needed for the refinement of the three ligands were built as described previously for reaction intermediate W.[24] Refinement statistics are included in Table S1. All the programs mentioned above, except *MXCuBe*, were provided by SBGrid.[25]

1.12 Molecular docking of 5MPzDC. The calculation was performed with the Schrödinger suite[26] using the X-ray model of the 6MPDC-containing *Tm*NadA*Y21F variant (Table S1). Hydrogen atoms were added to the model and protonation states were assigned using the standard protein preparation protocol of the Schrödinger suite. We used the protonated form of Glu195 because we previously found it to be the most likely state of this residue.[3] Next, water molecules present in the X-ray model were removed and the positions of the built hydrogen atoms were optimized. A receptor docking grid was defined by the 6MPDC ligand position. 6MPDC and 5MPzDC were prepared using the Ligprep program and then docked using the Glide program[26] with both the standard (SP) and the extra precision (XP) docking procedures. The X-ray position of 6MPDC was reproduced with the SP procedure (the pose was ranked 4th according to the docking score) but that was not the case with the XP procedure. When we superimposed the ligand-free *Tm*NadA*[13] (PDB code 4P3X) with the 6MPDC-containing *Tm*NadA*Y21F, the rmsd is 0.38 Å on all the protein atoms. Furthermore, we noticed that two water molecules (labeled 41 and 95 in our 6MPDC-NadA model) were also present in the ligand-free active site. A new docking grid was generated keeping these two water molecules in the target site. The pose with the best docking score (using either the SP or XP protocols) corresponded to the conformation of 6MPDC found in the X-ray structure. Accordingly, we decided to use this grid to also dock the 5MPzDC molecule. The docked poses indicate that there is a similar binding to the [4Fe-4S] cluster via the 5MPzDC thiolate. The pose with the highest docking score suggests that it should bind NadA as 6MPDC does (Figure S5). Figure S5 was prepared with Maestro from Schrödinger.[26]

2- Figures S1-S9

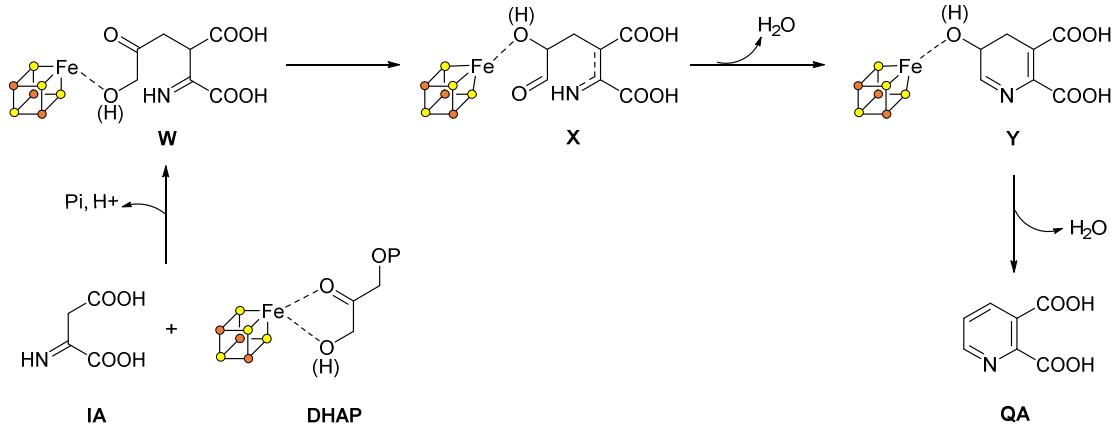

Fig. S1. Mechanism of QA synthesis by NadA based on previous studies.[3, 24, 27]

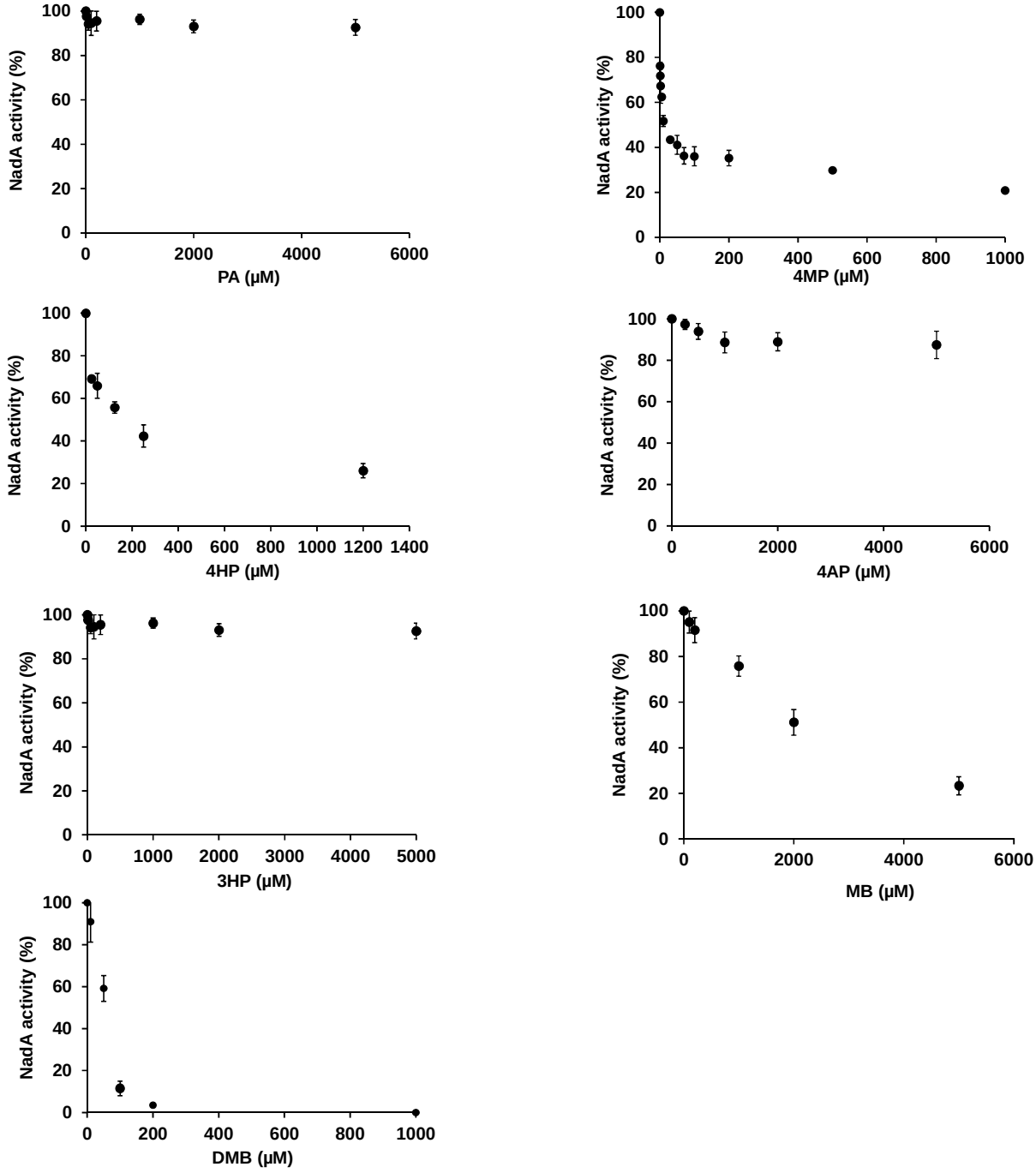

Fig. S2. NadA activity in the presence of PA, 4MP, 4HP, 4AP, 3HP, MB and DMB. [4Fe-4S]-*Ec*NadA (10 µM) was incubated 5 min. anaerobically with various equivalents of DTHPA derivatives in 50 mM Na-HEPES, 100 mM KCl, pH 7.5. The premix (2 mM DHAP, 33 mM L-aspartate, 25 mM fumarate) was added and after 5 min. incubation at 37°C the reaction was started by addition of *Ec*NadB (10 µM). After 20 min. the reaction was stopped and analyzed by HPLC.

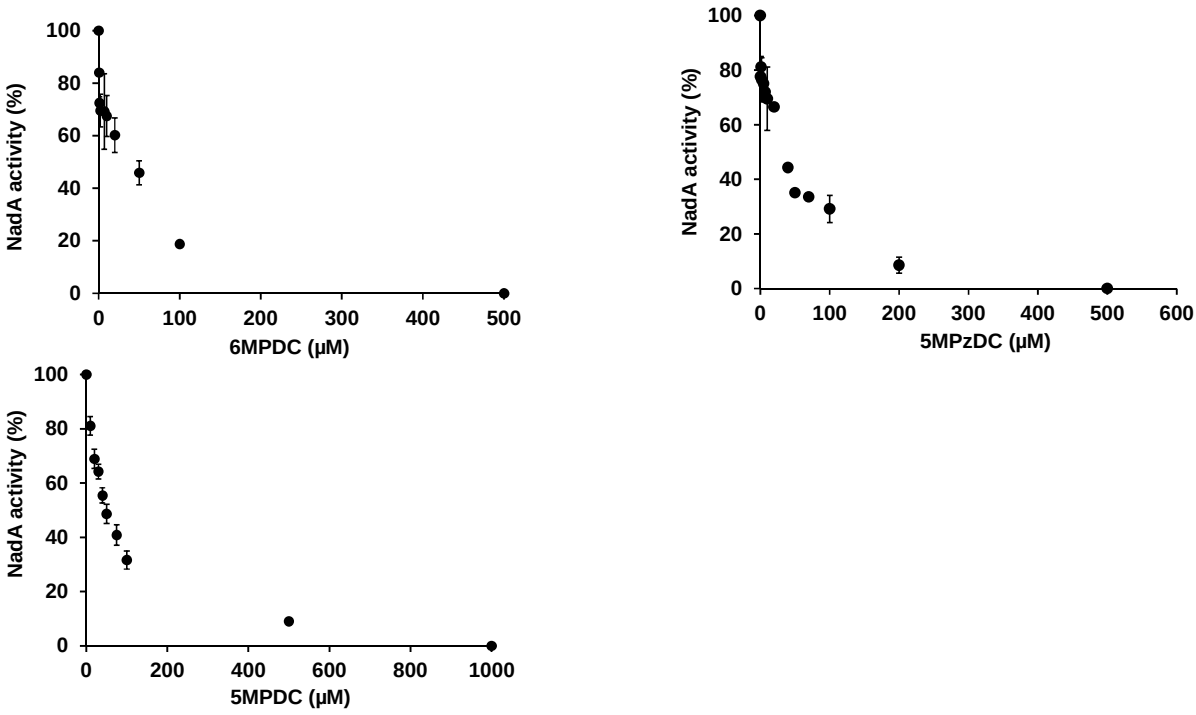

Fig. S3. NadA activity in the presence of 6MPDC, 5MPzDC and 5MPDC. [4Fe-4S]-*Ec*NadA (10 µM) was incubated 5 min. anaerobically with various equivalents of 6MPDC, 5MPzDC and 5MPDC in 50 mM Na-HEPES, 100 mM KCl, pH 7.5. The premix (2 mM DHAP, 33 mM L-aspartate, 25 mM fumarate) was added and after 5 min. incubation at 37°C the reaction was started by addition of *Ec*NadB (10 µM). After 20 min. the reaction was stopped and analyzed by HPLC.

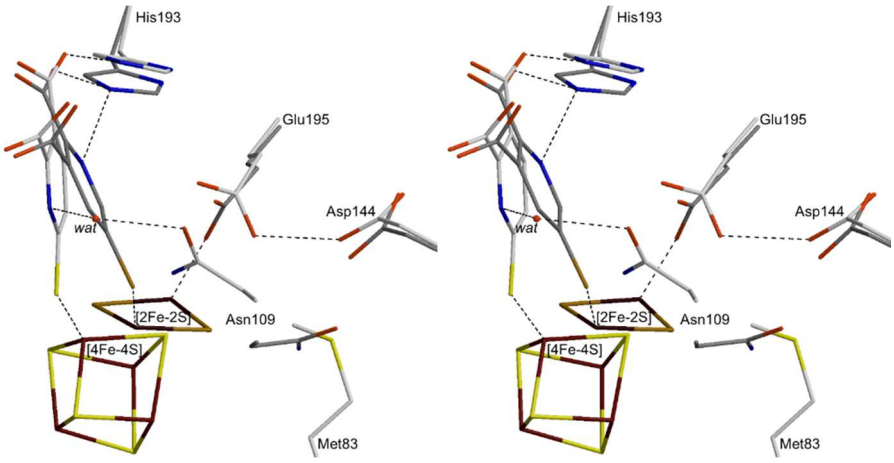

Fig. S4. Structure of *Tm*NadA* in complex with 6MPDC and 5MPDC. Stereo image of a superposition of 6MPDC (white carbons) and 5MPDC (grey carbons) complexes in an approximately perpendicular view relative to Figure 1 of the main text. Residues with significantly different conformations are highlighted. Only the [2Fe-2S] fragment is shown in the NadA-5MPDC complex.

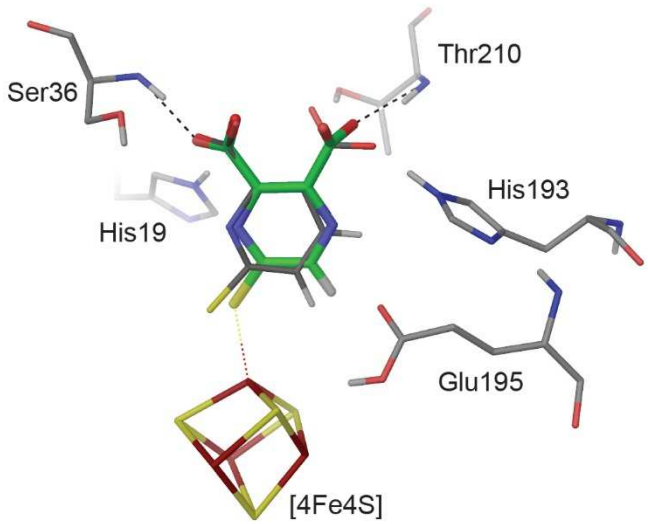

Fig. S5. Docking of 5MPzDC in *Tm*NadA*Y21F. The 5MPzDC molecule docked in *Tm*NadA*Y21F (best pose, carbon atoms in green) is compared to the conformation of 6MPDC in the X-ray structure (carbon atoms depicted in dark grey).

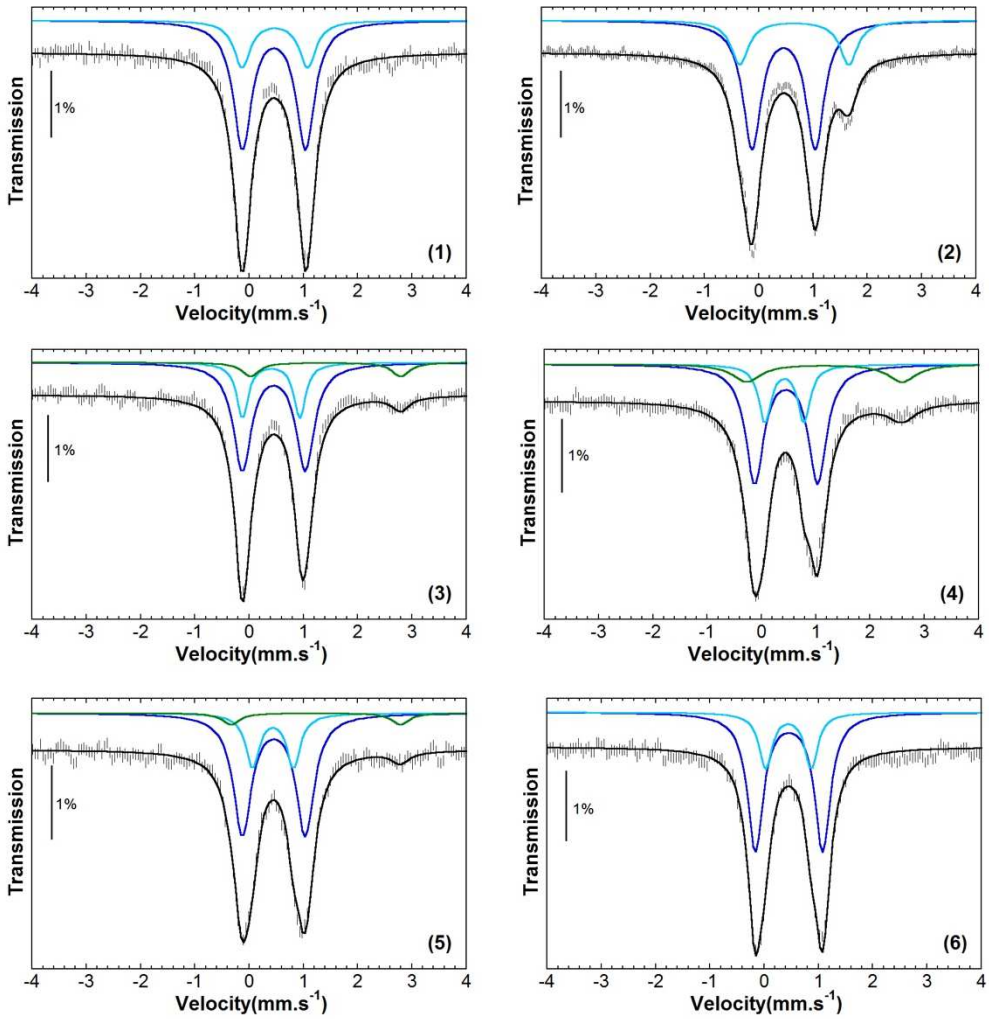

Fig. S6. Mossbauer spectra of *E. coli* ^{57}Fe-labeled [4Fe-4S]-*Ec*NadA (**1**) with 5-6 equiv. of DTHPA (**2**), 6MPDC (**3**); 5MPzDC (**4**); 5MPDC (**5**) and 4MP (**6**). The Mossbauer spectra were taken at 4.2 K with an external magnetic field of 0.06 T applied parallel to γ rays. Vertical bars: experimental points; solid line: simulations including black: overall simulation, blue: delocalized pair and cyan: "Fe^{2+}" site of the localized pair and green: Fe^{II} contaminant. Simulations were performed according to model (ii) (see paragraph 1.6) with the parameters listed in Table S2.

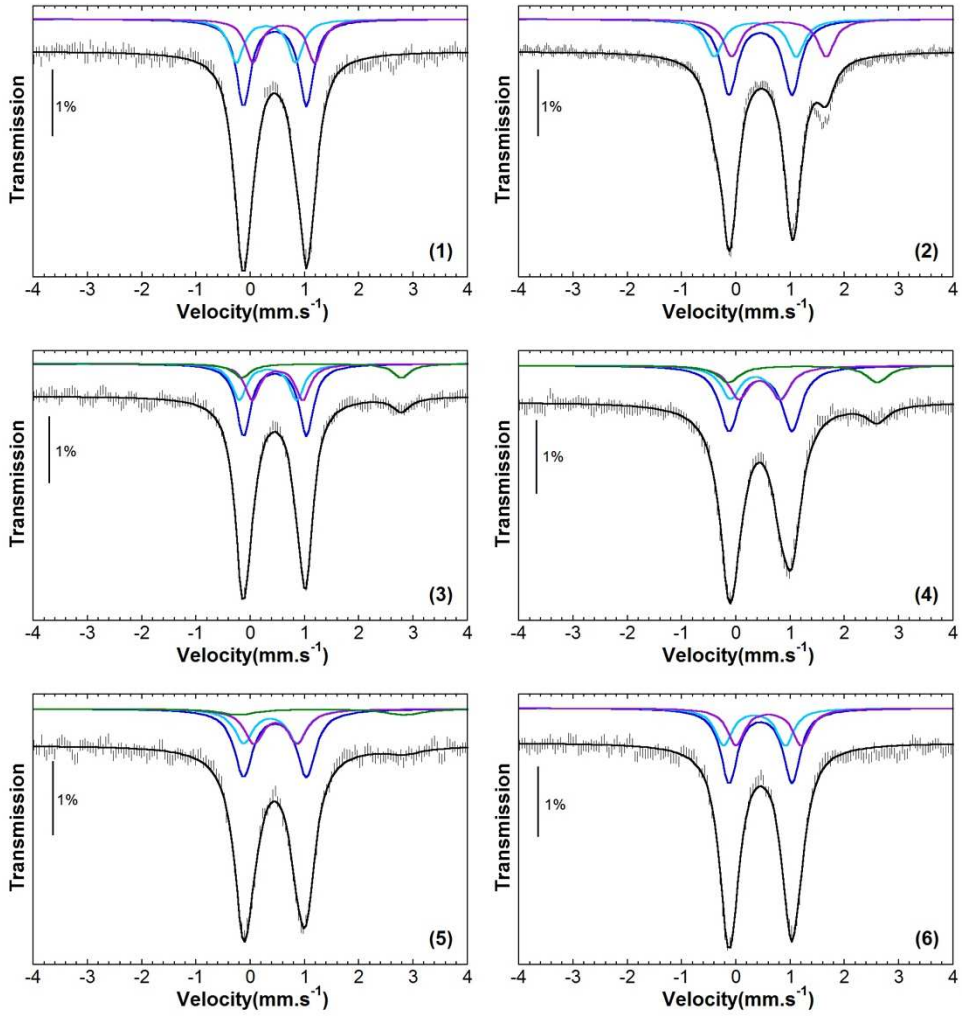

Fig. S7.
Mossbauer spectra of *E. coli* ^{57}Fe-labelled [4Fe-4S]-NadA (**1**) with 5-6 equiv. of DTHPA (**2**), 6MPDC (**3**); 5MPzDC (**4**); 5MPDC (**5**) and 4MP (**6**). The Mossbauer spectra were taken at 4.2 K with an external magnetic field of 0.06 T applied parallel to γ rays. Vertical bars: experimental points; solid line: simulations including black: overall simulation, blue: delocalized pair, cyan: "Fe^{3+}" site and purple: "Fe^{2+}" site of the localized pair and green: Fe^{II} contaminant. Simulations were performed according to model (iii) (see paragraph 1.6) with the parameters listed in Table S3.

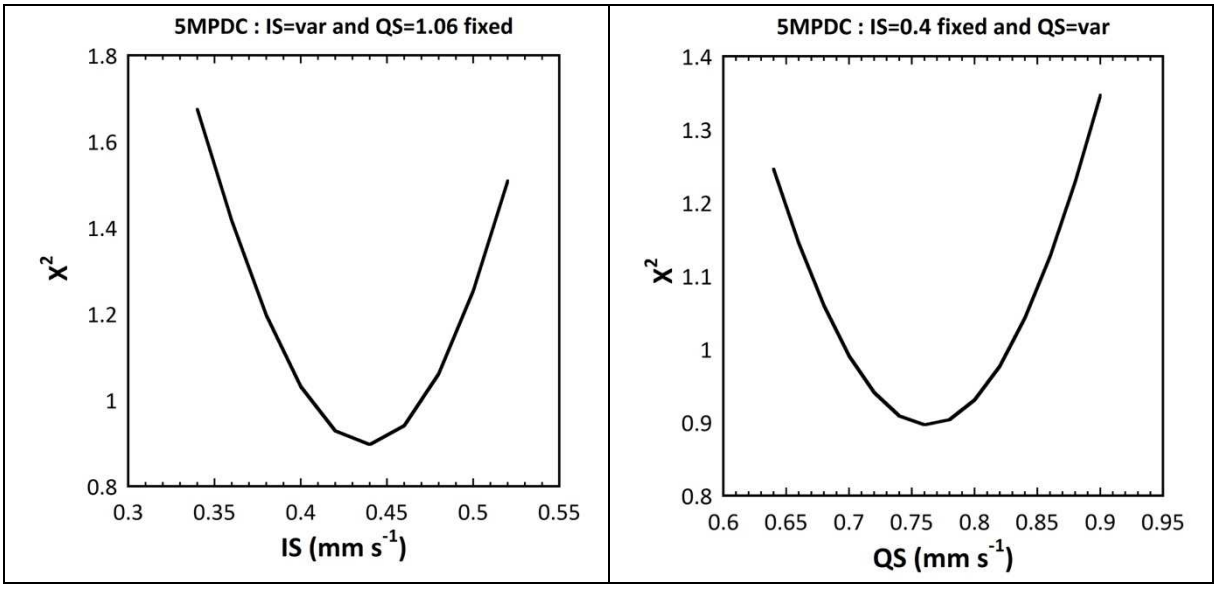

Fig. S8.
Analysis of Mossbauer parameters Isomer Shift (IS, left) and Quadrupole Splitting (QS, right) deduced from the simulation of the spectrum of ^{57}Fe-labelled [4Fe-4S]-*Ec*NadA with 5.7 equiv. of 5MPDC. The analysed data correspond to experimental and simulated spectra from Fig. S6 and Table S2.

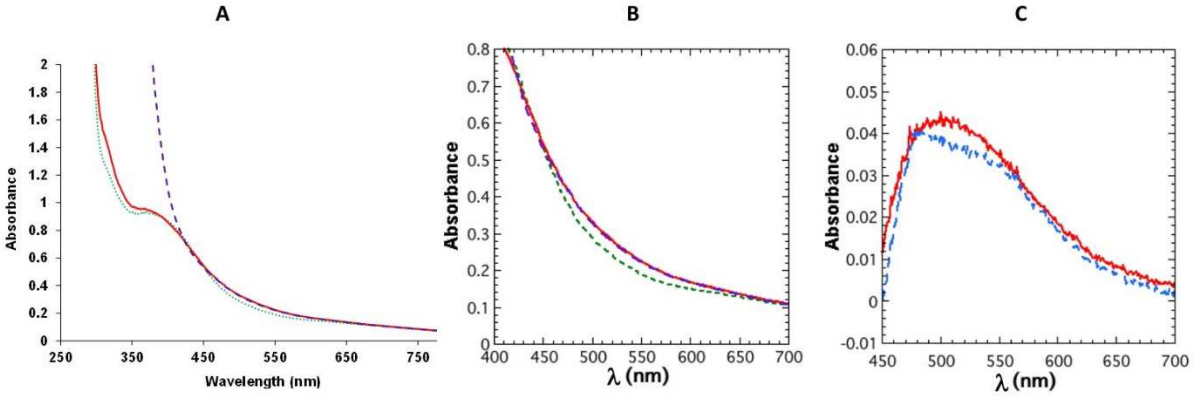

Fig. S9. UV-visible spectra of [4Fe-4S]-*Ec*NadA complexed with 6MPDC and 4MP. (A): [4Fe-4S]-*Ec*NadA (300 µM) UV-visible spectra before (green dotted line) and after addition and 15 min. incubation with 10 equiv. of 6MPDC (blue dashed line) and 4MP (red line). (B): focus of the 400-700 nm region of spectra presented in (A); (C): Gaussian simulations of 4MP (red line) and 6MPDC (blue line).

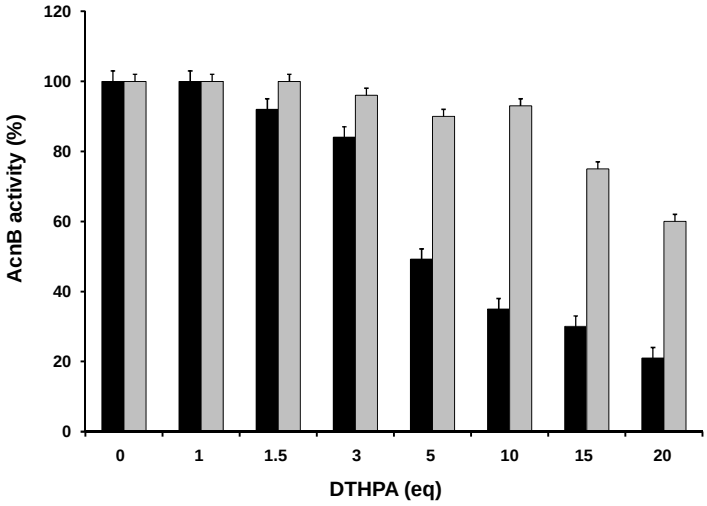

Fig. S10. Inhibition of [4Fe-4S]-*Ec*AcnB activity by DTHPA. [4Fe-4S]-*Ec*AcnB (3 µM) without (black bars) or with 3 µM [4Fe-4S]-*Ec*NadA (grey bars) was incubated 15 min. with DTHPA (0-20 equiv.) and its activity measured (n≥3).

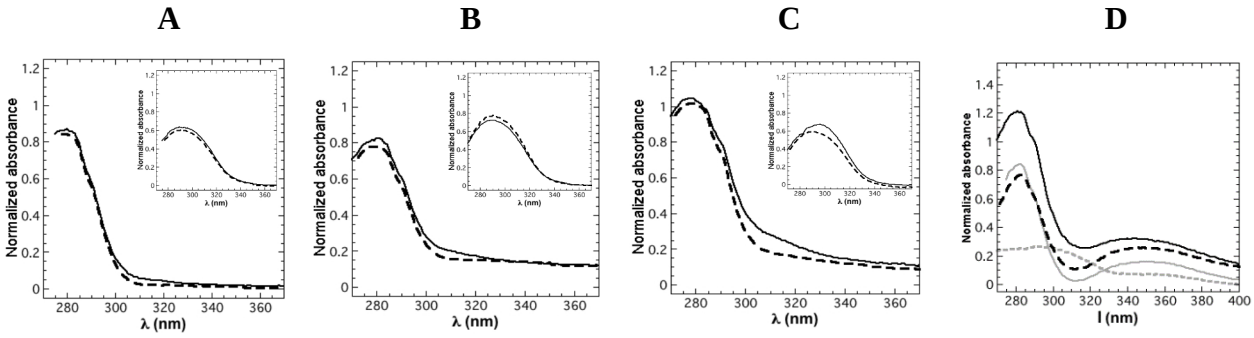

Fig. S11. UV-visible spectra of *Ec*NadA and *Ec*AcnB with 6MPDC and 4MP. Panels (A-C) depict the respective UV-visible spectra of Apo-*Ec*AcnB **(A)**, [4Fe-4S]-*Ec*AcnB **(B)** and [4Fe-4S]-*Ec*NadA **(C)** in the absence (dotted line) and presence of 5 equiv. of 4MP (solid line). Insets show the comparison between the spectrum of 4MP (5 equiv.) (dotted line) and the subtraction of the "(protein+4MP) - protein" (solid line) spectra. Panel **(D)** represents the UV-visible spectra of 6MPDC alone (– –), [4Fe-4S]-*Ec*NadA (—), [4Fe-4S]-*Ec*AcnB (- -) and ApoAcnB (—) in the presence of 6MPDC. A similar treatment of the data obtained with 6MPDC failed to reveal a specific interaction with the Fe-S clusters.

3- Tables S1-S4

Table S1. X-ray data and refinement statistics for *Tm*NadA*-Y21F crystals.

Complex	**4MP** pH 6.7	**6MPDC** pH 7.3	**5MPDC** pH 6.7
Data collection:			
ESRF beamline	ID29	ID30B [a]	ID30B [a]
Wavelength (Å)	1.07438	0.97625	1.00394
Space group	$P2_1$	$P2_1$	$P2_1$
Cell: a, b, c (Å)	55.7, 48.4, 60.6	55.5, 48.7, 60.6	54.9, 48.5, 60.5
Cell: β (°)	107.66	107.0	107.1
Resolution (Å)	46.8-1.60	46.5-1.90	37.2-2.10
high resolution shell [b]:	(1.66-1.60)	(1.97-1.90)	(2.17-2.10)
anisotropy along **a**, **b** and **c** (Å)	1.60 1.60 1.76	1.90 1.90 1.96	2.10 2.10 2.19
Measured reflections	176966 (18269)	141788 (12532)	50636 (4842)
Unique reflections	40160 (3936)	24522 (2390)	17011 (1670)
Redundancy	4.4 (4.6)	5.8 (5.2)	3.0 (2.9)
Completeness (%)	98.7 (99.5)	99.7 (99.7)	95.3 (96.7)
R_{merge} (%) [c]	7.6 (129.8)	10.9 (100.4)	11.7 (78.8)
$CC_{1/2}$	0.997 (0.314)	0.995 (0.573)	0.982 (0.536)
$\langle I/\sigma_I \rangle$	8.7 (1.0)	9.0 (1.5)	8.5 (1.4)
Refinement:			
Resolution (Å)	46.8-1.64	46.5-1.90	37.2-2.10
Used reflections	35414	23281	16177
R_{work} (%)	15.6	17.0	19.8
Reflections for R_{free}	1845	1227	830
R_{free} (%)	20.6	20.0	23.9
Number of atoms [d]	2717	2759	2543
Average B-factor (Å^2)	32.4	34.9	43.7
R.m.s. deviations			
Bond lengths (Å)	0.007	0.012	0.010
Bond angles (°)	1.4	1.5	1.5

[a] Diffraction data from two isomorphous crystals were merged; [b] the high resolution shell statistics are given in parentheses for all data; [c] treating Friedel pairs as different reflections; [d] including multiple conformations. Coordinates and structure factors have been deposited in the Protein Data Bank with deposition codes 6I0K (4MP complex), 6I0P (6MPDC complex) and 6I0R (5MPDC complex).

Table S2. Mossbauer parameters of ^{57}Fe-labeled [4Fe-4S]-*Ec*NadA (**1**) with 5-6 equiv. of DTHPA (**2**), 6MPDC (**3**); 5MPzDC (**4**); 5MPDC (**5**) and 4MP (**6**). Assignments: blue: delocalized pair; cyan: "Fe^{2+}" site of the localized pair and green: Fe^{II} contaminant.

Sample	*Molecule*	*Species*	δ (mm.s^{-1})	ΔE_Q (mm.s^{-1})	Γ (mm.s^{-1})	*Area (%)*
1	[4Fe-4S]-NadA	4Fe-4S	0.45	1.16	0.41	75
			0.47	1.21	0.37	25
2	DTHPA	4Fe-4S	0.45	1.16	0.41	75
			0.65	2.01	0.39	25
3	6MPDC	4Fe-4S	0.45	1.16	0.41	68
			0.40	1.06	0.26	23
		Fe^{II}	1.41	2.77	0.38	9
4	5MPzDC	4Fe-4S	0.45	1.16	0.41	64
			0.42	0.72	0.28	21
		Fe^{II}	1.16	2.86	0.63	15
5	5MPDC	4Fe-4S	0.45	1.16	0.41	70
			0.44	0.76	0.30	23
		Fe^{II}	1.23	3.12	0.38	6
6	4MP	4Fe-4S	0.45	1.16	0.41	75
			0.49	1.25	0.44	25

Table S3. Mossbauer parameters of ^{57}Fe-labeled [4Fe-4S]-*Ec*NadA (**1**) with 5-6 equiv. of DTHPA (**2**), 6MPDC (**3**); 5MPzDC (**4**); 5MPDC (**5**) and 4MP (**6**). Assignments: blue: delocalized pair, cyan: "Fe^{3+}" site and purple: "Fe^{2+}" site of the localized pair and green: Fe^{II} contaminant.

Sample	*Molecule*	*Species*	δ (mm.s^{-1})	ΔE_Q (mm.s^{-1})	Γ (mm.s^{-1})	*Area* (%)
1	[4Fe-4S]-NadA	4Fe-4S	0.45	1.16	0.33	50
			0.29	1.10	0.33	25
			0.61	1.14	0.33	25
2	DTHPA	4Fe-4S	0.45	1.16	0.37	50
			0.35	1.51	0.37	25
			0.79	1.74	0.37	25
3	6MPDC	4Fe-4S	0.45	1.16	0.32	45
			0.32	1.06	0.32	22
			0.50	0.94	0.32	22
		Fe^{II}	1.31	2.94	0.38	11
4	5MPzDC	4Fe-4S	0.45	1.16	0.43	44
			0.36	0.92	0.43	22
			0.43	0.77	0.43	22
		Fe^{II}	1.23	2.74	0.48	13
5	5MPDC	4Fe-4S	0.45	1.16	0.41	46
			0.37	0.99	0.41	23
			0.46	0.80	0.41	23
		Fe^{II}	1.30	3.06	0.80	8
6	4MP	4Fe-4S	0.45	1.16	0.38	50
			0.34	1.14	0.38	25
			0.60	1.21	0.38	25

Table S4. Energies* of the absorption maxima of solutions of 4MP in absence and in presence of proteins.

	4MP	4MP + protein	Energy difference
[4Fe-4S]-*Ec*AcnB	34.482	34.434	0.048
Apo-*Ec*AcnB	34.367	34.326	0.041
[4Fe-4S]-*Ec*NadA	34.405	34.010	0.395

* Energies are given in kilokaysers; 1 kK = 1 000 cm^{-1}.

References

1. J. E. Shaw, *Journal of Organic Chemistry*, 1991, **56**, 3728-3729.
2. A. Feretti, *Organic Syntheses*, 1962, **5**, 419.
3. A. Volbeda, J. S. Cabodevilla, C. Darnault, O. Gigarel, T. H. L. Han, O. Renoux, O. Hamelin, S. Agnier-de-Choudens, P. Amara and J. C. Fontecilla-Camps, *Acs Chemical Biology*, 2018, **13**, 1209-1217.
4. B. J. Knight, J. O. Rothbaum and E. M. Ferreira, *Chem Sci*, 2016, **7**, 1982-1987.
5. K. Yoshiizumi, M. Yamamoto, T. Miyasaka, Y. Ito, H. Kumihara, M. Sawa, T. Kiyoi, T. Yamamoto, F. Nakajima, R. Hirayama, H. Kondo, E. Ishibushi, H. Ohmoto, Y. Inoue and K. Yoshino, *Bioorg Med Chem*, 2003, **11**, 433-450.
6. 2013.
7. T. P. Holler, F. Q. Ruan, A. Spaltenstein and P. B. Hopkins, *Journal of Organic Chemistry*, 1989, **54**, 4570-4575.
8. C. A. Obafemi and W. Pfleiderer, *Helv Chim Acta*, 1994, **77**, 1549-1556.
9. C. Rousset, M. Fontecave and S. Ollagnier de Choudens, *FEBS Lett.*, 2008, **582**, 2937-2944.
10. A. Chan, M. Clemancey, J. M. Mouesca, P. Amara, O. Hamelin, J. M. Latour and S. Ollagnier de Choudens, *Angew Chem Int Ed Engl*, 2012, **51**, 7711-7714.
11. W. W. Fish, *Methods Enzymol*, 1988, **158**, 357-364.
12. H. Beinert, *Anal Biochem*, 1983, **131**, 373-378.
13. M. V. Cherrier, A. Chan, C. Darnault, D. Reichmann, P. Amara, S. Ollagnier de Choudens and J. C. Fontecilla-Camps, *J Am Chem Soc*, 2014, **136**, 5253-5256.
14. P. A. Jordan, Y. Tang, A. J. Bradbury, A. J. Thomson and J. R. Guest, *Biochem J*, 1999, **344 Pt 3**, 739-746.
15. P. R. Gardner and I. Fridovich, *J Biol Chem*, 1992, **267**, 8757-8763.
16. X. Vernede and J. C. Fontecilla-Camps, *J. Appl. Crystallogr.*, 1999, **32**, 505-509.
17. J. Gabadinho, A. Beteva, M. Guijarro, V. Rey-Bakaikoa, D. Spruce, M. W. Bowler, S. Brockhauser, D. Flot, E. J. Gordon, D. R. Hall, B. Lavault, A. A. McCarthy, J. McCarthy, E. Mitchell, S. Monaco, C. Mueller-Dieckmann, D. Nurizzo, R. B. G. Ravelli, X. Thibault, M. A. Walsh, G. A. Leonard and S. M. McSweeney, *J Synchrotron Radiat*, 2010, **17**, 700-707.
18. W. Kabsch, *Acta Crystallogr. Sect. D-Biol. Crystallogr.*, 2010, **66**, 125-132.
19. P. R. Evans and G. N. Murshudov, *Acta Crystallogr. Sect. D-Biol. Crystallogr.*, 2013, **69**, 1204-1214.
20. M. D. Winn, C. C. Ballard, K. D. Cowtan, E. J. Dodson, P. Emsley, P. R. Evans, R. M. Keegan, E. B. Krissinel, A. G. W. Leslie, A. McCoy, S. J. McNicholas, G. N. Murshudov, N. S. Pannu, E. A. Potterton, H. R. Powell, R. J. Read, A. Vagin and K. S. Wilson, *Acta Crystallogr. Sect. D-Biol. Crystallogr.*, 2011, **67**, 235-242.
21. A. J. Mccoy, R. W. Grosse-Kunstleve, P. D. Adams, M. D. Winn, L. C. Storoni and R. J. Read, *J. Appl. Crystallogr.*, 2007, **40**, 658-674.
22. P. Emsley, B. Lohkamp, W. G. Scott and K. Cowtan, *Acta Crystallogr.*, 2010, **D66**, 486-501.
23. G. N. Murshudov, P. Skubak, A. A. Lebedev, N. S. Pannu, R. A. Steiner, R. A. Nicholls, M. D. Winn, F. Long and A. A. Vagin, *Acta Crystallogr. Sect. D-Biol. Crystallogr.*, 2011, **67**, 355-367.
24. A. Volbeda, C. Darnault, O. Renoux, D. Reichmann, P. Amara, S. Ollagnier de Choudens and J. C. Fontecilla-Camps, *J Am Chem Soc*, 2016, **138**, 11802-11809.
25. A. Morin, B. Eisenbraun, J. Key, P. C. Sanschagrin, M. A. Timony, M. Ottaviano and P. Sliz, *Elife*, 2013, **2**.
26. S. Schrödinger Release 2016-1:Jaguar, LCC, New York, NY, 2016.

27. D. Reichmann, Y. Coute and S. Ollagnier de Choudens, *Biochemistry*, 2015, **54**, 6443-6446.